Title

Inhibition of CSF-1 Receptor Improves the Antitumor Efficacy of Adoptive Cell Transfer Immunotherapy

Permalink

https://escholarship.org/uc/item/2vr0c2r7

Authors

Mok, Stephen
Koya, Richard C
Tsui, Christopher
et al.

Peer reviewed

Inhibition of CSF1 Receptor Improves the Anti-tumor Efficacy of Adoptive Cell Transfer Immunotherapy

Stephen Mok[#][a], **Richard C. Koya**[#][h], **Christopher Tsui**[d], **Jingying Xu**[a], **Lídia Robert**[i], **Lily Wu**[a,d,e,f], **Thomas Graeber**[a,b,d,g], **Brian L. West**[h], **Gideon Bollag**[h], and **Antoni Ribas**[a,b,c,d,i]

[a]Department of Molecular and Medical Pharmacology, University of California Los Angeles, 10833 Le Conte Avenue, Los Angeles, CA 90095 (UCLA)

[b]the Jonsson Comprehensive Cancer Center (JCCC) at UCLA

[c]Surgery, Division of Surgical Oncology, UCLA

[d]Institute for Molecular Medicine, UCLA

[e]Department of Urology, UCLA

[f]Department of Pediatrics, UCLA

[g]Crump Institute for Molecular Imaging, UCLA

[h]Plexxikon Inc., Berkeley, California 94710, U.S.A; Roswell Park Cancer Institute, Buffalo, New York 14263

[i]Department of Medicine, Division of Hematology/Oncology, UCLA

[#] These authors contributed equally to this work.

Abstract

Colony stimulating factor-1 (CSF-1) recruits tumor-infiltrating myeloid cells (TIMs) that suppress tumor immunity, including M2 macrophages and myeloid derived suppressor cells (MDSC). The CSF-1 receptor (CSF-1R) is a tyrosine kinase that is targetable by small molecule inhibitors such as PLX3397. In this study, we used a syngeneic mouse model of BRAFV600E-driven melanoma to evaluate the ability of PLX3397 to improve the efficacy of adoptive T-cell therapy (ACT). In this model, we found that combined treatment produced superior anti-tumor responses compared with single treatments. In mice receiving the combined treatment, a dramatic reduction of TIMs and a skewing of MHCII^{low} to MHCII^{hi} macrophages was observed. Further, mice receiving the combined treatment exhibited an increase in tumor-infiltrating lymphocytes (TILs) and T cells, as revealed by real-time imaging in vivo. In support of these observations, TILs from these mice released higher levels of IFN-γ. In conclusion, CSF-1R blockade with PLX3397 improved the efficacy of ACT immunotherapy by inhibiting the intratumoral accumulation of immune suppressive macrophages.

Keywords

melanoma; adoptive cell transfer; CSF-1R; PLX3397; myeloid cells

Corresponding Authors: Richard C. Koya, M.D., Ph.D., Roswell Park Cancer Institute, Elm & Carlton Streets, Buffalo, NewYork 14263, Telephone: 716-845-1300, ext. 6582, Richard.Koya@RoswellPark.org. Antoni Ribas, MD, Ph.D., Division of Hematology-Oncology, 11-934 Factor Building, 10833 Le Conte Avenue, Los Angeles, CA 90095-1782, USA. Telephone: 310-206-3928. Fax: 310-825-2493. aribas@mednet.ucla.edu..

Introduction

Established solid tumors consist of both transformed neoplastic cells and non-transformed host cells such as stromal cells, lymphocytes, dendritic cells, macrophages, and MDSC. In order to escape immune responses, tumor cells manipulate the surrounding tumor microenvironment by producing cytokines that suppress cytolytic T-cells and recruit immune suppressive cells (1-3). CSF-1 is a cytokine frequently produced by several cancers, including melanoma (4, 5). The secreted CSF-1 binds to the tyrosine kinase receptor CSF-1R on the myeloid cells, which results in increased proliferation and differentiation of myeloid cells into type M2 macrophages and MDSC, and their recruitment into tumors (6, 7). The M2-polarized macrophages and MDSC use several mechanisms to induce an immune suppressive tumor environment, such as the release of arginase I or inducible nitric oxide synthase (iNOS), leading to T-cell inhibition (1). Therefore, an immune suppressive tumor milieu mediated by CSF-1 may limit the anti-tumor activity of tumor immunotherapy and lead to low response rates (3).

In prior studies, we have established a $BRAF^{V600E}$ mutant murine melanoma cell line, SM1, to provide a relevant model of melanoma in fully syngeneic immunocompetent mice (8). $BRAF^{V600E}$ is the driver oncogene in approximately 50% of human melanomas (9). Besides being driven by the $BRAF^{V600E}$ oncogene, SM1 has multiple genomic aberrations in a pattern similar to 108 human melanoma cell lines based on results of high-density single nucleotide polymorphism (SNP)/copy number alteration (CNA) arrays. It includes amplification of oncogenic $BRAF^{V600E}$ and of the microphthalmia-associated transcription factor (MITF), and a deletion of $CDKN2A$. In the SM1 model, adoptive cell transfer (ACT) of melanoma targeted T-cells induces anti-tumor responses that are enhanced by the addition of the BRAF inhibitor vemurafenib (8). In addition, this same mouse model has been used to test the anti-tumor effects of several immune modulating antibodies, including anti-CTLA4, anti-PD-1, anti-Tim3 and agonistic anti-CD137 (41BB) (10). Only anti-CD137 had significant anti-tumor activity alone or in combination with BRAF inhibitor therapy, suggesting that there may be factors in the tumor microenvironment that inhibit the effector arm of the immune system.

PLX3397 is a potent tyrosine kinase inhibitor (TKI) selected for its ability to inhibit CSF-1R. It is currently in clinical development as a single agent or in combination therapy for the treatment of patients with glioblastoma (GBM), breast cancer, and other cancers through its inhibition of the CSF-1R, and also acute myelogenous leukemia through its inhibition of FLT3-ITD. In preclinical models, CSF-1R inhibitors including PLX3397 have been reported to inhibit the immune suppressive tumor milieu and facilitate immune responses to cancer (11-14). We hypothesized that a combination of PLX3397 and ACT immunotherapy would improve the tumor microenvironment through the inhibition of immunosuppressive myeloid cells resulting in better T cell antitumor functions. Our results demonstrate significantly enhanced efficacy of the combined treatment, mediated by decreasing TIMs and increasing activated TILs compared with either of the single treatment groups.

Materials and Methods

Mice, Cell Lines and Reagents

C57BL/6 mice, OT-1 transgenic mice (Jackson Laboratories, Bar Harbor, ME), pmel-1 (Thy1.1) transgenic mice (kind gift from Dr. Nicholas Restifo, Surgery Branch, National Cancer Institute, Bethesda, MD), and NOD/SCID/γ chain[null] (NSG) mice (NOD.Cg-$Prkdc$[scid]$Il2rg$[tm1Wjl]/SzJ, Jackson Laboratory, Bar Harbor, ME) were bred and kept under defined-flora pathogen-free conditions at the AALAC-approved animal facility of the

Division of Experimental Radiation Oncology, UCLA, and used under the UCLA Animal Research Committee protocol #2004-159. The B16 murine melanoma cell line was obtained from ATCC (Rockville, MD) and maintained in DMEM (Mediatech, Inc., Herndon, VA) with 10% FCS (Omega Scientific, Tarzana, CA) and 1% penicillin, streptomycin, and amphotericin (Omega Scientific). The SM1 murine melanoma was generated from a spontaneously arising tumor in *BRAF*^{V600E} mutant transgenic mice as previously described (15). SM1 was maintained in RPMI (Mediatech, Herndon, VA) with 10% FCS (Omega Scientific), 2 mM L-glutamine (Invitrogen, Carlsbad, CA) and 1% penicillin, streptomycin and amphotericin. SM1-OVA was generated by stable expression of OVA through lentiviral transduction as previously described (15). PLX3397 was obtained under a materials transfer agreement (MTA) with Plexxikon Inc. (Berkeley, CA). PLX3397 was dissolved in dimethyl sulfoxide (DMSO, Fisher Scientific, Morristown, NJ). For *in vivo* studies, PLX3397 was dissolved in DMSO, and then a suspension made by dilution into an aqueous mixture of 0.5% hydroxypropyl methyl cellulose (HPMC) and 1% polysorbate (PS80) (Sigma-Aldrich). 100 µL of the suspended drug was administered by daily oral gavage into mice at 50 mg/kg when tumors reached 3 mm in diameter. For macrophage depletion studies, 1 mg of clodronate (Clodrosome, Nashville, TN) was injected i.p. every 5 days. For antibody-mediated depletion studies, 250 µg of anti-CD8 antibody, 200 µg of anti-CSF-1 or isotype control antibody (BioXCell, West Lebanon, NH) was injected i.p. every 3 days.

Cell Viability Assays

Murine melanoma cells (5×10^3 cells/well) and activated C57BL/6 splenocytes (5×10^4 cells/well) were seeded on 96-well flat-bottom plates with 100 µL of 10% FCS media and incubated for 24 hours. Graded dilutions of PLX3397 or DMSO vehicle control, in culture medium, were added to each well in triplicate and analyzed by using tetrazolium compound [3-(4,5-dimethylthiazol-2-yl)-5-(3-carboxymethoxyphenyl-2-(4-sulfophenyl)-2H-tetrazolium (MTS)-based colorimetric cell proliferation assay (Promega, Madison, WI).

Adoptive Cell Transfer (ACT) Therapy *In Vivo* Models

B16, SM1-OVA or SM1 cells were implanted s.c. in C57BL/6 mice, and when tumors reached 5 mm in diameter, mice were conditioned for ACT with a lymphodepleting regimen of 500 cGy of total body irradiation (TBI). Then they received 2×10^5 or 1×10^6 OVA$_{257-264}$ peptide-activated OT-1 splenocytes or gp100$_{25-33}$ peptide-activated pmel-1 splenocytes intravenously (i.v.) as previously described (15). In both cases, the ACT was followed by three days of daily i.p. administration of 50,000 IU of IL-2. Tumors were followed by caliper measurements three times per week.

Flow Cytometry Analysis

SM1 tumors, lungs, blood, bone marrow, and spleens were harvested from mice. Tumors and lungs were further digested with collagenase (Sigma-Aldrich). TIMs obtained from digested SM1 tumors, were stained with antibodies to Gr-1, CD11b, F4/80, MHCII (eBiosciences) and Ly6C (BD Biosciences). Tumor infiltrating lymphocytes were stained with antibodies with CD3, Thy1.1 (BD Biosciences), CD4, and CD8 (eBiosciences) and analyzed with a LSR-II or FACSCalibur flow cytometers (BD Biosciences), followed by Flow-Jo software (Tree-Star, Ashland, OR) analysis as previously described (16). Intracellular interferon gamma (IFN-γ) staining was done as previously described (16).

Immunofluorescence Imaging

Staining was performed as previously described (15). Briefly, sections of OCT (Sakura Finetek, Torrance, CA) cryopreserved tissues were blocked in donkey serum/ PBS and incubated with primary antibodies to Gr-1 (BD Biosciences) or F4/80 (Abcam), followed by

secondary donkey anti-rat antibodies conjugated to DyLight488 (Jackson Immunoresearch Laboratories, West Grove, PA). Negative controls consisted of isotype matched rabbit or rat IgG in lieu of the primary antibodies listed above. DAPI (4,6-diamidino-2-phenylindole) was used for the visualization of nuclei. Immunofluorescence images were taken in a fluorescence microscope (Axioplan-2; Carl Zeiss Microimaging, Thornwood, NY).

Bioluminescence imaging (BLI)

OT-1 or pmel-1 splenocytes were retrovirally-transduced to express firefly luciferase as previously described (15), and used for ACT. BLI was performed with a Xenogen IVIS 200 Imaging System (Xenogen/Caliper Life Sciences, Hopkinton, MA) as previously described (15).

Statistical analysis

Data were analyzed with GraphPad Prism (version 5) software (GraphPad Software, La Jolla, CA). A Mann-Whitney test or ANOVA with Bonferroni post-test was used to analyze experimental data. Survival curves were generated by actuarial Kaplan–Meier method and analyzed with the Jump-In software (SAS) with log-rank test for comparisons from the time of tumor challenge to when mice were sacrificed due to tumors reaching 14 mm in maximum diameter, or the end of the study period had been reached.

Results

PLX3397 does not have direct cytotoxic effects against SM1 and preserves splenocytes

We tested the effects of single agent PLX3397 against SM1 using an *in vitro* MTS cell proliferation assay after 72 hours of exposure to rule out a potential direct anti-tumor effect of this CSF-1R inhibitor in the SM1 murine melanoma cell line. An IC_{50} was not reached even at 1 μM (Fig. 1a). In addition to its resistance in MTS assays, exposure of SM1 to PLX3397 at the range of concentrations between 10 nM and 1 μM showed no inhibition of the downstream MAPK signaling pathway (Fig. 1b). SM1 does not express either CSF-1R or c-kit by FACS analysis and gene expression profiling (data not shown); these are the two main targets of PLX3397. SM1 also produces high levels of CSF-1 protein and its level is not affected by PLX3397 at 1 μM (Supplemental Fig. 1). We then ruled out that PLX3397 had a potential detrimental effect against T-cells. Increasing concentrations of PLX3397 did not negatively alter the viability of murine splenocytes after 72 hours of treatment (Fig. 1c). In contrast, 1 μM of PLX3397 was enough to down-regulate pErk level and to kill cells that were dependent on CSF-1/CSF-1R for growth such as myeloid cells and microglia cells (12, 17). Therefore, since single agent PLX3397 did not affect the viability of either SM1 cells or murine splenocytes, this supports SM1 as a permissive model for testing the effects of PLX3397 to improve the anti-tumor activity of ACT immunotherapy.

Combined therapy with PLX3397 and ACT immunotherapy improves anti-tumor responses against SM1 tumors

Lymphodepleted C57BL/6 mice with established subcutaneous SM1-OVA tumors received ACT of splenocytes obtained from OT-1 mice expressing an OVA-specific TCR. We titrated the application of immunotherapy to provide a suboptimal anti-tumor effect that was similar to the anti-tumor effect of single agent PLX3397 so that the effect of combination could be revealed (Fig. 2a). The combined therapy of PLX3397 and OT-1 TCR transgenic ACT demonstrated superior anti-tumor effects compared to either therapy alone in duplicate experiments and improved overall survival (Fig. 2b; Supplemental Fig. 2a). As the OVA model is based on the recognition of a foreign antigen, we further confirmed the results in the pmel-1 ACT model that is based on transgenic T-cells with a TCR recognizing gp100, a

murine melanosomal antigen endogenously expressed by SM1 (8) (Fig. 2c). In replicate studies, the combined therapy with pmel-1 ACT and PLX3397 also had superior anti-tumor response compared with either single agent therapy alone and improved survival (Fig. 2d; Supplemental Fig. 2a). To also test the general applicability of combining PLX3397 and pmel-1 ACT, another murine melanoma model, B16 was used. Combined therapy also demonstrated superior anti-tumor response compared to either therapy alone in duplicate experiments (Supplemental Fig. 2b).

Decrease in tumor infiltrating macrophages by inhibition of CSF-1R by PLX3397

To analyze whether PLX3397 changed the magnitude of TIMs, including macrophages and MDSC, we analyzed their presence in tumors by immunofluorescence. There was a decrease in the quantity of F4/80(+) macrophages in both the PLX3397 single agent group and the combined group compared to vehicle or ACT single treatment groups (Fig. 3a). Analysis of tumors, spleens, lungs, blood, and bone marrow from mice treated with PLX3397 demonstrated that the effects of PLX3397 were specific for intratumoral macrophages as opposed to a systemic depletion of macrophages. There was a local (tumor) decrease in quantity of F4/80(+) CD11b(+) macrophages but no significant decrease systemically (Fig. 3b and 3d; Supplemental Fig. 3). To further characterize the phenotype of the remaining macrophages, MHCII expression was analyzed by FACS. There was a shift in macrophage phenotype from MHCII^{low} to MHCII^{hi} upon treatment with PLX3397 (Fig. 3c and 3d; Supplemental Fig. 3).

No difference in MDSC number and ratio of PMN/MO-MDSC in combined treatment of ACT with PLX3397

The level of MDSC in SM1 tumors was first analyzed by immunofluorescence. The MDSCs were present at a low level in tumors and their level appeared to be unaltered by ACT or PLX3397 treatment (Fig. 4a). To better enumerate the magnitude and distribution of MDSC *in vivo*, we analyzed their presence in tumors, spleens, lungs, blood, and bone marrow by flow cytometry. Confirming the immunofluorescence data, there was no change in the already low (~4-6%) baseline quantity of Gr-1(+) CD11b(+) MDSC following treatment with PLX3397 (Fig. 4b and 4d; Supplemental Fig. 3). We then examined whether PLX3397 altered the ratio between the two recognized subsets of MDSCs, the polymorphonuclear MDSC (PMN-MDSC, Gr-1^{hi} Ly6C^{low}) and the monocytic MDSCs (MO-MDSC, Gr-1^{low} Ly6C^{hi}). There was no significant difference between PLX3397 treated and non-treated groups in MDSC subsets, just as there was no change in total MDSCs (Fig. 4c and 4d; Supplemental Fig. 3).

Effect of CSF-1 or macrophage depletion overlapped with the effects of PLX3397

In order to confirm the role of CSF-1 in the activity of PLX3397, PLX3397 treatment was combined with anti-CSF-1 antibody in mice that received ACT with pmel-1 splenocytes. There was no improvement in anti-tumor activity in the PLX3397, pmel-1 ACT and anti-CSF-1 antibody treatment groups, compared to mice receiving PLX3397 and pmel-1 ACT therapy with an isotype control antibody (Fig. 5a), suggesting that the effects of PLX3397 and anti-CSF-1 antibody-mediated depletion might be overlapping. To determine if the target of PLX3397 was macrophages, mice with established SM1 tumors were treated with PLX3397 in combination with clodronate, an agent that depletes macrophages. There was no enhanced anti-tumor response in the combined treatment group of PLX3397 and clodronate compared with either single treatment group (Fig. 5b). These studies suggest that PLX3397 mediated its effects through inhibition of immune suppressive CSF-1-responding intratumoral macrophages.

PLX3397 increases the expansion, distribution, and functional activation of intratumoral lymphocytes

To analyze whole animal T-cell distribution in the presence or absence of PLX3397, we genetically labeled the adoptively transferred OT-1 T-cells with firefly luciferase transgene for *in vivo* bioluminescence imaging. There was an increased expansion, *in vivo* distribution to tumor, and tumor targeting by adoptively transferred OT-1 T-cells when mice were treated with PLX3397 (Fig. 6a). The quantitative analysis of T-cell-associated luciferase activity in mice treated with OT-1 ACT combined with PLX3397 showed increased accumulation within OVA antigen-matched tumors over time (Fig. 6b; Supplemental Fig. 4a). Further, we repeated the bioluminescence imaging using pmel-1 T-cells also labeled with the firefly luciferase transgene and used for ACT. Again, PLX3397 increased the expansion of pmel-1 T-cells distributed to gp100 positive antigen-matched SM1 tumors (Fig. 6c). Mice that received pmel-1 ACT combined with PLX3397 also demonstrated an increased intratumoral accumulation of luciferase activity to tumors over time (Fig. 6d; Supplemental Fig. 4b). We then analyzed the activation state of TILs by detecting cytokine production. In two replicate experiments, TILs collected from mice treated with the combination of pmel-1 ACT and PLX3397 showed a higher ability to secrete IFN-γ and to respond to short term *ex vivo* restimulation with the gp100 antigen (Fig. 6e). Therefore, treatment with PLX3397 increased both the number and functionality of adoptively transferred anti-tumor antigen-specific T-cells.

The anti-tumor activity of PLX3397 is T-cell-dependent

Single agent PLX3397 treatment demonstrated a weak but reproducible anti-tumor response compared with vehicle control (Fig. 2b, 2c, and 5b). We tested if this antitumor activity was mediated by endogenous cytotoxic CD8 T-cells. SM1 tumors were implanted in C57BL/6 mice without irradiation and received PLX3397 in combination with anti-CD8 antibody. The depletion of CD8+ cells abrogated the antitumor activity of single agent PLX3397 (Fig. 7a). To further test the role of immune cells in the antitumor activity of PLX3397, immunodeficient NSG mice were implanted with SM1 tumors and dosed with PLX3397. In these immunodeficient mice there was no anti-tumor activity of PLX3397 compared to mice receiving vehicle control (Fig. 7b). Finally, we tested whether the anti-tumor effects of PLX3397 was also dependent on cytotoxic CD8 T-cells in the pmel-1 ACT model. C57BL/6 mice with established SM1 tumors were treated with a combination of PLX3397, anti-CD8 antibody, and pmel-1 ACT. There was no anti-tumor activity of pmel-1 ACT combined with PLX3397 in mice that received CD8 depleting antibody (Fig. 7c). Collectively, these studies highlight the role of CD8+ T-cells as effectors of the antitumor activity of PLX3397 in the SM1 murine melanoma model.

Discussion

Tumor immunotherapy with cytokines such as interferon or IL-2, immune modulating antibodies blocking the cytotoxic T leukocyte-associated antigen-4 (CTLA4) or the programmed cell death receptor 1 (PD-1) or its ligand PD-L1, and the adoptive transfer of tumor antigen-specific T-cells, result in tumor responses in patients with advanced cancers, and melanoma in particular. These immunotherapy-induced tumor responses are frequently extremely durable and can last years. However, their low response rate has been one of the obstacles remaining to overcome (3, 18). A potential explanation is that intratumoral immune suppressive myeloid cells may inhibit immunotherapy responses via different mechanisms (1). These myeloid lineage cells represent various distinct and heterogeneous populations of immune suppressive cells including MDSC and macrophages. By suppressing these myeloid cells with CSF-1R blockade using PLX3397, we hypothesized that T-cell function within tumors may improve. Hence, the ideal treatment would be to

suppress the myeloid cells and increase the number of effector T-cells at the same time. SM1 tumors grow very rapidly when implanted in C57BL/6 mice, such that mice often need to be sacrificed within two to three weeks of tumor implantation, limiting the ability to induce an immune response with immune modulating antibodies (8, 10). To overcome this, and provide the opportunity for a fully effective immune response in combination with CSF-1R blockade, we have used the ACT of T-cells expressing TCRs recognizing a specific tumor antigen on the tumor cells. The scientific rationale posits that inhibition of CSF-1R signaling in immune suppressive TIMs will improve the intratumoral milieu by taking away immune suppressive factors that limit the anti-tumor activity of cytotoxic T lymphocytes (CTLs).

We explored the potential mechanisms by which PLX3397 improves the anti-tumor effect of ACT. The myeloid cells infiltrating SM1 tumors are mainly macrophages. Our data demonstrate that PLX3397 decreases the quantity of macrophages locally in tumor. Although the classification between M1 and M2 polarized macrophages is still controversial, MHCII is used as a marker to distinguish them (19). With PLX3397 there is a skewing of the population of MHCII^{low} to MHCII^{hi} macrophages, consistent with a previous report (13). By decreasing the presence of immune suppressive MHCII^{low} macrophages, PLX3397 likely facilitates the intratumoral trafficking of adoptively transferred lymphocytes and their anti-tumor functions. Our studies also suggest that macrophage inhibition alone by PLX3397 is not sufficient for an anti-tumor response. An immune response is indeed needed for the anti-tumor effect of PLX3397 in the SM1 model since this effect requires CD8 T-cells. Therefore, the main beneficial effects of PLX3397 in this model are derived from the ability to improve T cell effector functions indirectly through the inhibition of intratumoral immune suppressive macrophages.

Reports have shown that different tumor models such as prostate and lung carcinoma models are MDSC-dominant and these MDSC are heavily infiltrated in tumors and systemic organs such as spleen, blood, and bone marrow (14, 20). By contrast, our SM1 model has few MDSC infiltrating the tumor or accumulated in the spleen over time. This is consistent with a recent report that shows patients with melanoma have far less MDSC than other cancers and also compared to many non-melanoma murine tumor models (21). In addition, prior reports have shown that CSF-1R blockade therapy reduced the number of myeloid cells including MDSC and macrophages in both tumors and systemic organs (4, 14). In contrast, in our model CSF-1R blockade with PLX3397 mainly targeted the more abundant macrophages instead of MDSC suggesting the role of CSF-1 may be tumor model-dependent. Different tumor models, genetic backgrounds, or treatments may induce different growth factors or cytokines in the tumor microenvironment. As myeloid cell tumor infiltration is a complex process regulated by different pathways, it is possible that different tumor models and tumors from different patients producing different cytokines like CSF-1, IL-34 or CCL2 result in attraction of different myeloid lineages leading to differential responses to CSF-1R blockade (22-25). For example, it has been reported that under hypoxic conditions induced expression of HIF-1α results in the expression of CXCR4 and SDF-1. The SDF-1/CXCR4 axis is another pathway that mediates the recruitment of TIMs to tumors (26, 27). Future immunotherapy trials may thus benefit from molecular profiling-based stratification of patients in regards to their tumor microenvironment cytokines.

In conclusion, combined therapy with the CSF-1R inhibitor PLX3397 and TCR-based ACT immunotherapy results in superior anti-tumor effects than single agent treatment in a murine model of melanoma. The anti-tumor activity is mediated by inhibition of the myeloid cell-mediated immunosuppressive tumor microenvironment so that more lymphocytes infiltrate into the tumor with enhanced functionality.

Supplementary Material

Refer to Web version on PubMed Central for supplementary material.

Acknowledgments

Reference

1. Gabrilovich DI, Nagaraj S. Myeloid-derived suppressor cells as regulators of the immune system. Nat Rev Immunol. 2009; 9:162–174. [PubMed: 19197294]

2. Schreiber RD, Old LJ, Smyth MJ. Cancer immunoediting: integrating immunity's roles in cancer suppression and promotion. Science. 2011; 331:1565–1570. [PubMed: 21436444]

3. Kerkar SP, Restifo NP. Cellular constituents of immune escape within the tumor microenvironment. Cancer Res. 2012; 72:3125–3130. [PubMed: 22721837]

4. Priceman SJ, Sung JL, Shaposhnik Z, Burton JB, Torres-Collado AX, Moughon DL, Johnson M, Lusis AJ, Cohen DA, Iruela-Arispe ML, et al. Targeting distinct tumor-infiltrating myeloid cells by inhibiting CSF-1 receptor: combating tumor evasion of antiangiogenic therapy. Blood. 2010; 115:1461–1471. [PubMed: 20008303]

5. Tarhini AA, Butterfield LH, Shuai Y, Gooding WE, Kalinski P, Kirkwood JM. Differing patterns of circulating regulatory T cells and myeloid-derived suppressor cells in metastatic melanoma patients receiving anti-CTLA4 antibody and interferon-alpha or TLR-9 agonist and GM-CSF with peptide vaccination. J Immunother. 2012; 35:702–710. [PubMed: 23090079]

6. Dai XM, Ryan GR, Hapel AJ, Dominguez MG, Russell RG, Kapp S, Sylvestre V, Stanley ER. Targeted disruption of the mouse colony-stimulating factor 1 receptor gene results in osteopetrosis, mononuclear phagocyte deficiency, increased primitive progenitor cell frequencies, and reproductive defects. Blood. 2002; 99:111–120. [PubMed: 11756160]

7. Li J, Chen K, Zhu L, Pollard JW. Conditional deletion of the colony stimulating factor-1 receptor (c-fms proto-oncogene) in mice. Genesis. 2006; 44:328–335. [PubMed: 16823860]

8. Koya RC, Mok S, Otte N, Blacketor KJ, Comin-Anduix B, Tumeh PC, Minasyan A, Graham NA, Graeber TG, Chodon T, et al. BRAF Inhibitor Vemurafenib Improves the Antitumor Activity of Adoptive Cell Immunotherapy. Cancer Res. 2012; 72:3928–3937. [PubMed: 22693252]

9. Gray-Schopfer V, Wellbrock C, Marais R. Melanoma biology and new targeted therapy. Nature. 2007; 445:851–857. [PubMed: 17314971]

10. Knight DA, Ngiow SF, Li M, Parmenter T, Mok S, Cass A, Haynes NM, Kinross K, Yagita H, Koya RC, et al. Host immunity contributes to the anti-melanoma activity of BRAF inhibitors. J Clin Invest. 2013; 123:1371–1381. [PubMed: 23454771]

11. Chitu V, Nacu V, Charles JF, Henne WM, McMahon HT, Nandi S, Ketchum H, Harris R, Nakamura MC, Stanley ER. PSTPIP2 deficiency in mice causes osteopenia and increased differentiation of multipotent myeloid precursors into osteoclasts. Blood. 2012

12. Coniglio SJ, Eugenin E, Dobrenis K, Stanley ER, West BL, Symons MH, Segall JE. Microglial stimulation of glioblastoma invasion involves epidermal growth factor receptor (EGFR) and colony stimulating factor 1 receptor (CSF-1R) signaling. Mol Med. 2012; 18:519–527. [PubMed: 22294205]

13. DeNardo DG, Brennan DJ, Rexhepaj E, Ruffell B, Shiao SL, Madden SF, Gallagher WM, Wadhwani N, Keil SD, Junaid SA, et al. Leukocyte complexity predicts breast cancer survival and

functionally regulates response to chemotherapy. Cancer Discov. 2011; 1:54–67. [PubMed: 22039576]

14. Xu J, Escamilla J, Mok S, David J, Priceman SJ, West BL, Bollag G, McBride WH, Wu L. Abrogating the protumorigenic influences of tumor-infiltrating myeloid cells byCSF1R signaling blockade improves the efficacy of radiotherapy in prostatecancer. Cancer Res. 2013

15. Koya RC, Mok S, Comin-Anduix B, Chodon T, Radu CG, Nishimura MI, Witte ON, Ribas A. Kinetic phases of distribution and tumor targeting by T cell receptor engineered lymphocytes inducing robust antitumor responses. Proc Natl Acad Sci U S A. 2010; 107:14286–14291. [PubMed: 20624956]

16. Vo DD, Prins RM, Begley JL, Donahue TR, Morris LF, Bruhn KW, de la Rocha P, Yang MY, Mok S, Garban HJ, et al. Enhanced antitumor activity induced by adoptive T-cell transfer and adjunctive use of the histone deacetylase inhibitor LAQ824. Cancer Res. 2009; 69:8693–8699. [PubMed: 19861533]

17. He Y, Rhodes SD, Chen S, Wu X, Yuan J, Yang X, Jiang L, Li X, Takahashi N, Xu M, et al. c-Fms signaling mediates neurofibromatosis Type-1 osteoclast gain-in-functions. PLoS One. 2012; 7:e46900. [PubMed: 23144792]

18. McArthur GA, Ribas A. Targeting oncogenic drivers and the immune system in melanoma. J Clin Oncol. 2013; 31:499–506. [PubMed: 23248252]

19. Gabrilovich DI, Ostrand-Rosenberg S, Bronte V. Coordinated regulation of myeloid cells by tumours. Nat Rev Immunol. 2012; 12:253–268. [PubMed: 22437938]

20. Srivastava MK, Zhu L, Harris-White M, Kar U, Huang M, Johnson MF, Lee JM, Elashoff D, Strieter R, Dubinett S, et al. Myeloid suppressor cell depletion augments antitumor activity in lung cancer. PLoS One. 2012; 7:e40677. [PubMed: 22815789]

21. Gros A, Turcotte S, Wunderlich JR, Ahmadzadeh M, Dudley ME, Rosenberg SA. Myeloid cells obtained from the blood but not from the tumor can suppress T-cell proliferation in patients with melanoma. Clin Cancer Res. 2012; 18:5212–5223. [PubMed: 22837179]

22. Lin H, Lee E, Hestir K, Leo C, Huang M, Bosch E, Halenbeck R, Wu G, Zhou A, Behrens D, et al. Discovery of a cytokine and its receptor by functional screening of the extracellular proteome. Science. 2008; 320:807–811. [PubMed: 18467591]

23. Wei S, Nandi S, Chitu V, Yeung YG, Yu W, Huang M, Williams LT, Lin H, Stanley ER. Functional overlap but differential expression of CSF-1 and IL-34 in their CSF-1 receptor-mediated regulation of myeloid cells. J Leukoc Biol. 2010; 88:495–505. [PubMed: 20504948]

24. Sawanobori Y, Ueha S, Kurachi M, Shimaoka T, Talmadge JE, Abe J, Shono Y, Kitabatake M, Kakimi K, Mukaida N, et al. Chemokine-mediated rapid turnover of myeloid-derived suppressor cells in tumor-bearing mice. Blood. 2008; 111:5457–5466. [PubMed: 18375791]

25. Li X, Loberg R, Liao J, Ying C, Snyder LA, Pienta KJ, McCauley LK. A destructive cascade mediated by CCL2 facilitates prostate cancer growth in bone. Cancer Res. 2009; 69:1685–1692. [PubMed: 19176388]

26. Kozin SV, Kamoun WS, Huang Y, Dawson MR, Jain RK, Duda DG. Recruitment of myeloid but not endothelial precursor cells facilitates tumor regrowth after local irradiation. Cancer Res. 2010; 70:5679–5685. [PubMed: 20631066]

27. Kioi M, Vogel H, Schultz G, Hoffman RM, Harsh GR, Brown JM. Inhibition of vasculogenesis, but not angiogenesis, prevents the recurrence of glioblastoma after irradiation in mice. J Clin Invest. 2010; 120:694–705. [PubMed: 20179352]
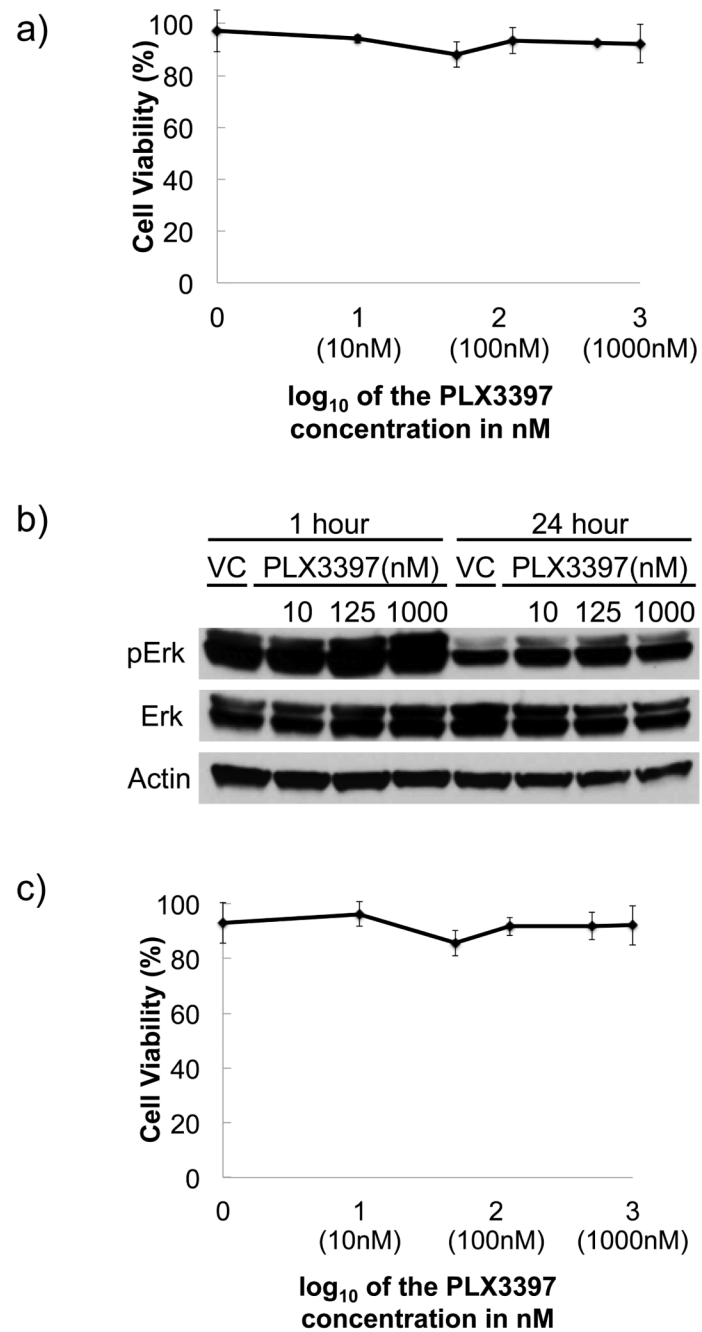
Figure 1. Effects of PLX3397 on SM1 melanoma and primary T-cells
a) Murine SM1 melanoma cells were exposed to increasing concentrations of PLX3397 for 72 hours for IC_{50} determination using an MTS assay. **b)** Immunoblotting for analysis of signaling molecules after PLX3397 exposure of SM1 cells at 10, 125, 1000 nM for 1 or 24 hours. **c)** Effects of PLX3397 on murine splenocyte viability. Cell viability assay (MTS) of *ex vivo* activated C57BL/6 splenocytes at 72 hour time point with increasing doses of PLX3397.
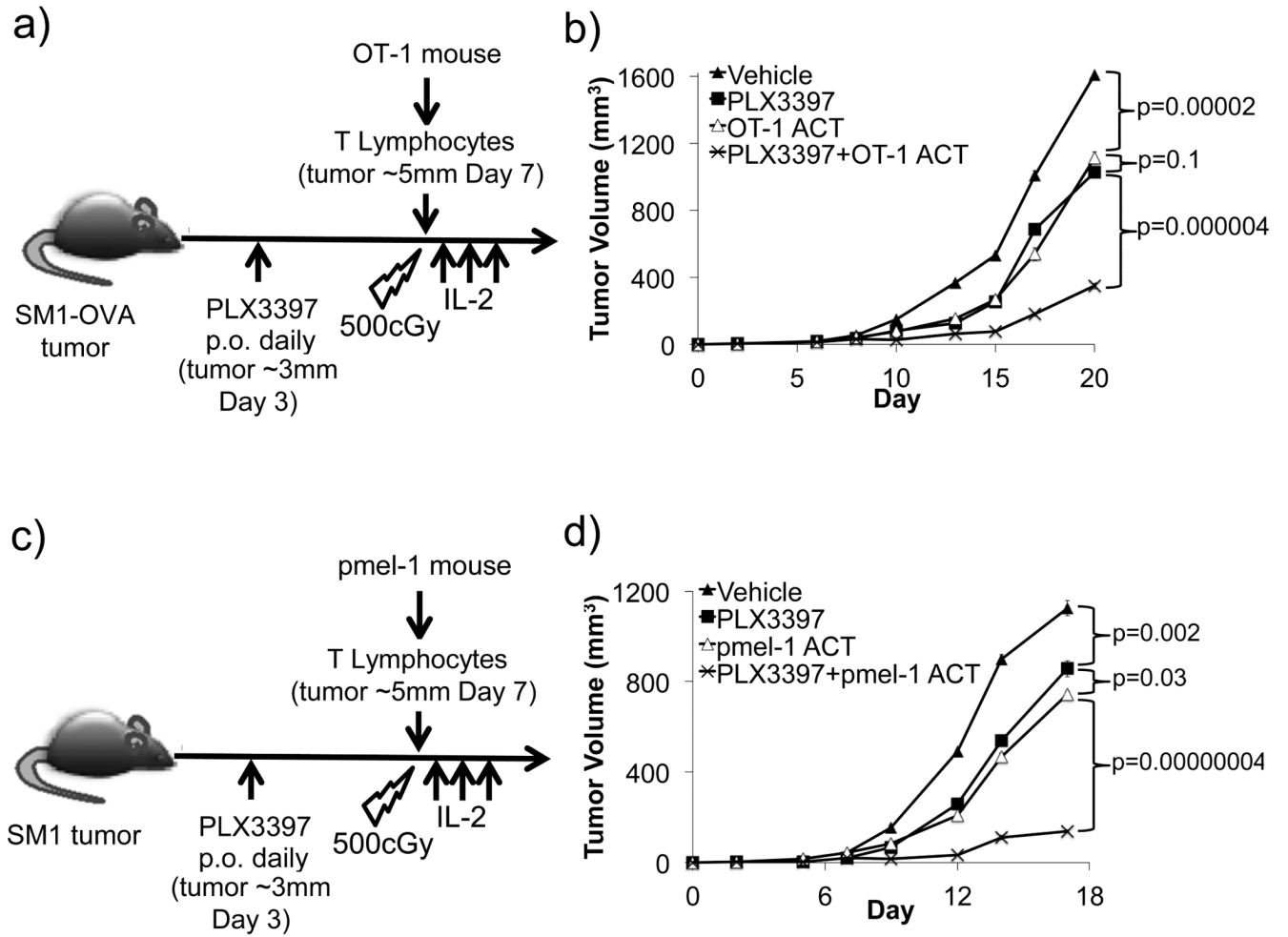
Figure 2. Combined anti-tumor activity of adoptive cell transfer (ACT) immunotherapy and PLX3397 in the ovalbumin (OVA) and pmel-1 models
a) Schematic of the OT-1 ACT model based on adoptively transferring OT-1 splenocytes into lymphodepleted mice with previously established SM1 tumors stably expressing OVA antigen (SM1-OVA). **b)** Tumor growth curves of established SM1-OVA tumors in C57BL/6 mice through day 20 post-tumor implantation. **c)** Schematic of pmel-1 ACT model with lymphdepleted mice harboring SM1 tumors that adoptively received pmel-1 splenocytes and PLX3397. **d)** Tumor growth curves of established SM1 tumors in C57BL/6 mice through day 18.
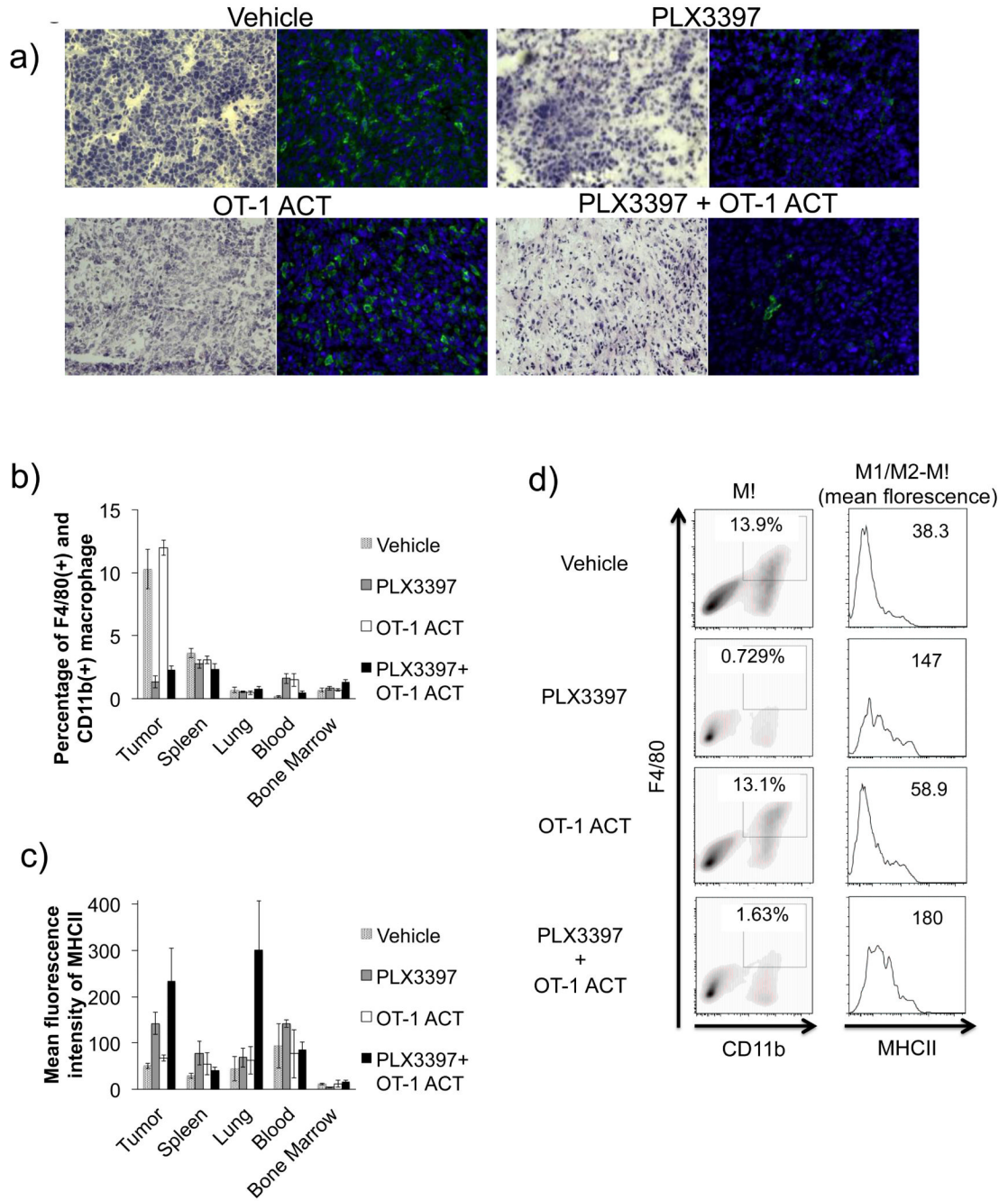
Figure 3. Changes in intratumoral macrophages in responses to PLX3397

C57BL/6 mice with SM1-OVA tumors were gavaged p.o. daily with PLX3397 and received OT-1 ACT for 18 days to assess prolonged effects of the drug on macrophages. **a)** Tissue immunofluorescence microscopy to detect macrophages. Representative H&E (left) and immunofluorescence for macrophages stained with anti-F4/80-FITC (green, right), and nuclei stained with DAPI (blue, right). **b)** Cells stained for the surface expression markers of macrophages (F4/80+ CD11b+), M1-macrophage (MHCII^{hi}), and M2-macrophage (MHCII^{low}) were used for FACS analysis. Bar-graph representation of percentage of F4/80(+) and CD11b(+) macrophages. **c)** Bar-graph representation of mean fluorescence intensity of MHCII expression on macrophages. **d)** Representative FACS plots

demonstrating percentage of F4/80(+) CD11b(+) macrophages and mean fluorescence intensity of M1-marophage (MHCII^{hi}) and M2-macrophage (MHCII^{low}) in tumor tissue.
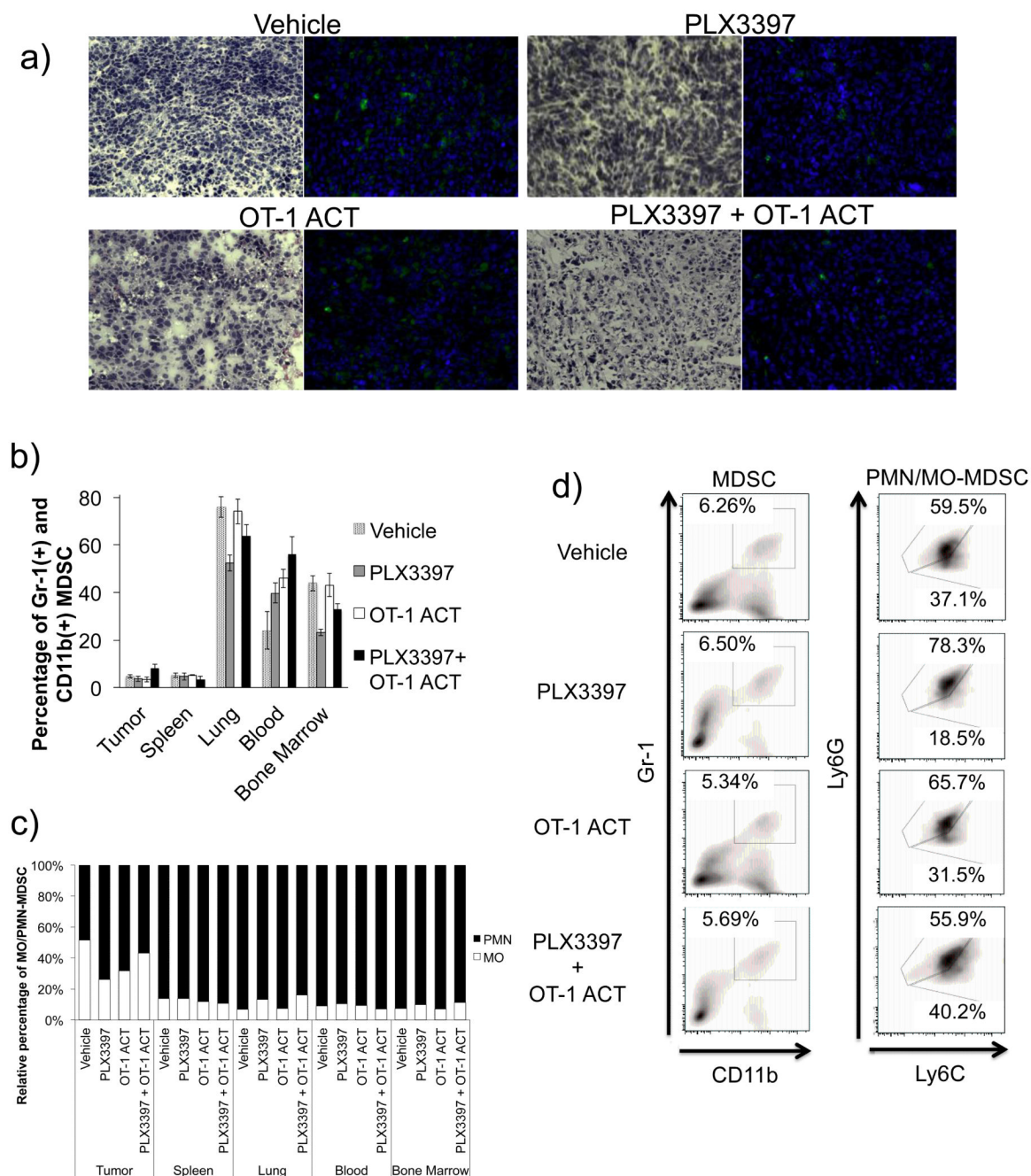
Figure 4. Analysis of MDSC with PLX3397 exposure

C57BL/6 mice with SM1-OVA tumors were gavaged p.o. daily with PLX3397 and received OT-1 ACT for 18 days to assess prolonged effects of the drug on MDSC. **a)** Tissue immunofluorescence microscopy to detect MDSC on day 14 post-ACT. Representative H&E (left) and immunofluorescence for MDSC stained with anti-Gr-1-FITC (green, right), and nuclei stained with DAPI (blue, right). **b)** Cells stained for the surface expression markers of MDSC (Gr-1+ CD11b+), MO-MDSC (Gr-1^{low} Ly6C^{hi}), and PMN-MDSC (Gr-1^{hi} Ly6C^{low}) were used for FACS analysis. Bar-graph representation of percentage of Gr-1(+) CD11b(+) MDSC. **c)** Bar-graph representation of ratio between MO-MDSC and

PMN-MDSC. **d)** Representative FACS plots demonstrating percentages of Gr-1(+) CD11b(+) MDSC, MO-MDSC (Gr-1^{low} Ly6C^{hi}), and PMN-MDSC (Gr-1^{hi} Ly6C^{low}) in tumor tissue.
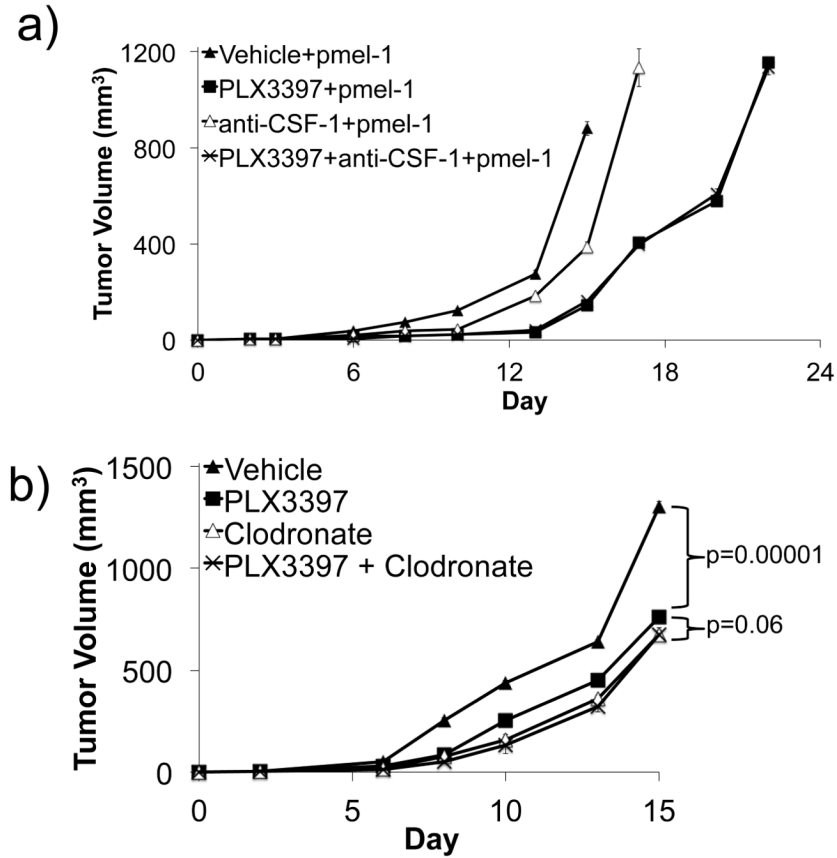
Figure 5. Effects of PLX3397 mediated by CSF-1R and macrophages
a) Tumor growth curves of established SM1 tumors in C57BL/6 mice that received pmel-1 ACT with PLX3397, and anti-CSF-1 antibody. Treatment of anti-CSF-1 or isotype antibody control was started at the same time with PLX3397 when the tumor diameter reached 3 mm. On day 15, between vehicle+pmel-1 and anti-CSF-1+pmel-1, p=0.000008; between anti-CSF-1+pmel-1 and PLX3397+pmel, p=0.00003; between PLX3397+pmel-1 and PLX3397+anti-CSF-1+pmel-1, p=0.1 **b)** Tumor growth curves of established SM1 tumors in C57BL/6 mice treated PLX3397 in combination with clodronate. Clodronate treatment was started at the same time with PLX3397 when the tumor diameter reached 3 mm.
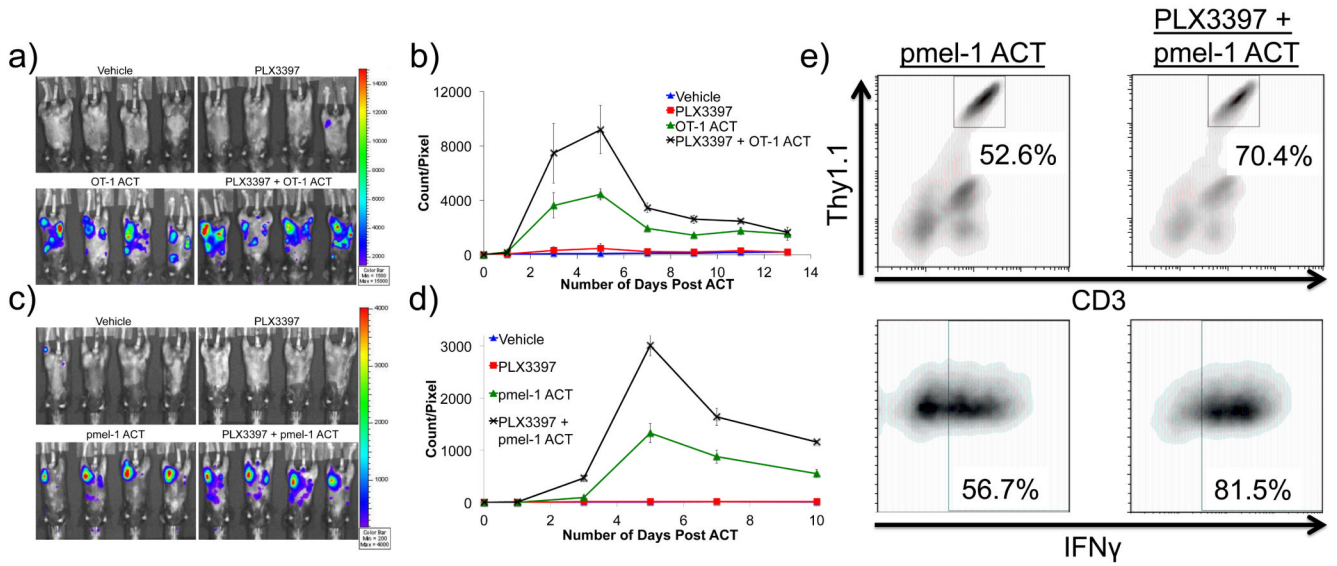
Figure 6. Effects of PLX3397 on the distribution and cytokine-producing functions of adoptively transferred lymphocytes

a) *In vivo* bioluminescence imaging of TCR transgenic T-cell distribution. OT-1 transgenic T-cells were transduced with a retrovirus-firefly luciferase and used for ACT. Representative figure at day 5 depicting 4 replicate mice per group. **b)** Quantitation of bioluminescence imaging of serial images with region of interest (ROI) analysis at the site of tumors obtained through day 13 post-ACT of OT-1 transgenic T-cells expressing firefly luciferase with 4 mice per group. **c)** Pmel-1 transgenic T-cells transduced with retrovirus-firefly luciferase were used for ACT. Day 5 representative figure showing 4 replicate mice per group. **d)** Quantitative measure of bioluminescence imaging signal with ROI at the tumor site obtained through day 10 post-ACT of luciferase expressing pmel-1 T-cells. **e)** Effects on cytokine production upon antigen restimulation. SM1 tumor-bearing C57BL/6 mice received pmel-1 ACT with or without PLX3397. At day 5 post-ACT, TILs were isolated for intracellular IFN-γ staining analyzed by FACS after 5 hour *ex vivo* exposure to the gp100$_{25\text{-}33}$ peptide.
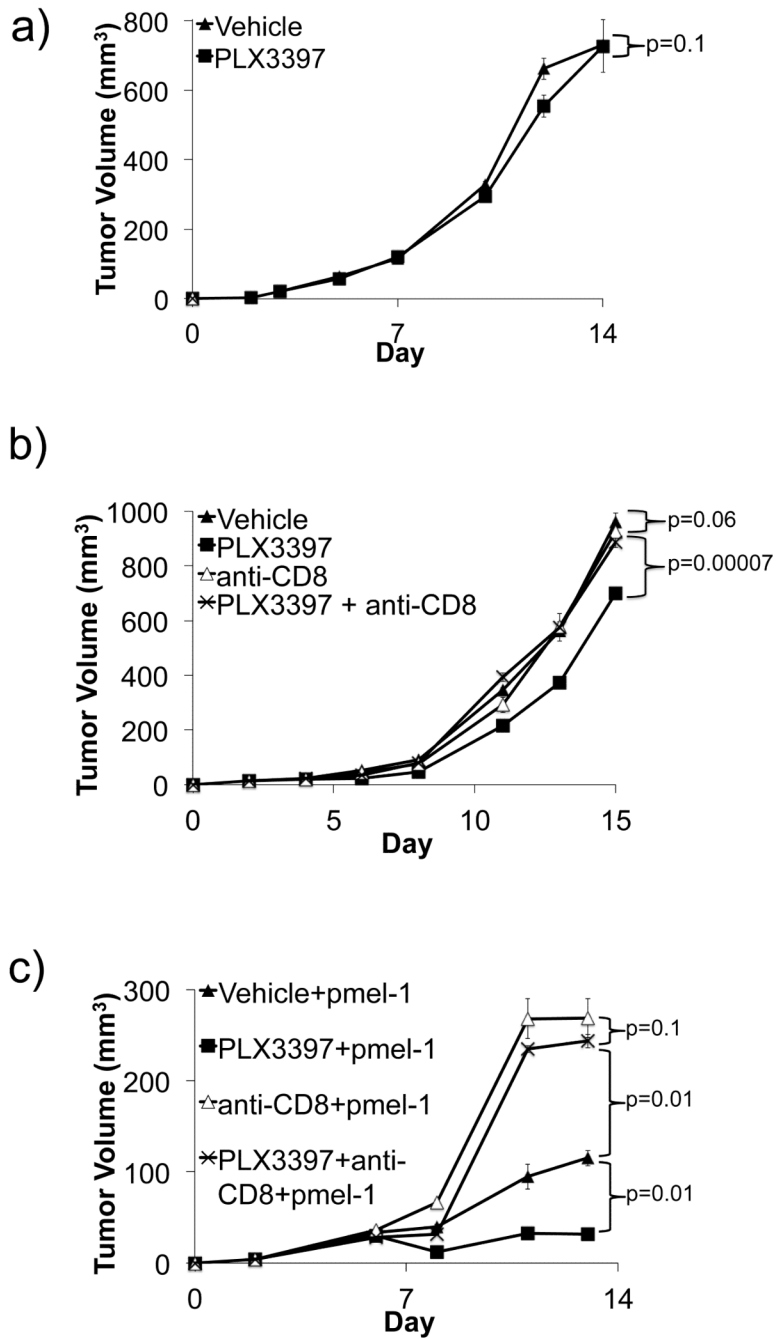
Figure 7. Lack of anti-tumor activity of PLX3397 in immunodeficient mice or with CD8+ T-cell depletion
a) Tumor growth curves of established SM1 tumors in non-irradiated C57BL/6 mice treated with PLX3397 in combination with anti-CD8 antibody. **b)** Tumor growth curves of established SM1 tumors in NSG mice treated with or without PLX3397. **c)** SM1 tumor-bearing mice received pmel-1 ACT and were treated with PLX3397 and anti-CD8 depleting antibody.